INSTITUTE OF PLASMA PHYSICS

NAGOYA UNIVERSITY

RESEARCH REPORT

NAGOYA, JAPAN

Nonlinear Magnetosonic Waves Propagating in a Magnetic Neutral Sheet

Jun-ichi Sakai

IPPJ-139 October 1972

Further communication about this report is to be sent to the Research Information Center, Institute of Plasma Physics, Nagoya University, Nagoya, Japan.

Abstract

Nonlinear magnetosonic waves propagating in a magnetic neutral sheet are investigated within the framework of a fluid model. It is shown that the behavior of the magnetosonic waves are governed by a 'modified Burgers equation' with an additional term $c(\eta)\phi$ due to the relevant slowly varying background plasma parameter (density or magnetic field),

$$\frac{\partial \phi}{\partial \eta} + a(\eta)\phi\frac{\partial \phi}{\partial \xi} - b(\eta)\frac{\partial^2 \phi}{\partial \xi^2} + c(\eta)\phi = 0,$$

where $\phi(\xi,\eta)$ is the amplitude of the magnetosonic waves, $\xi = \int k_x dx + k_y y - \omega t$, and $\eta = \varepsilon x$ is the coordinate stretched by a smallness parameter ε. When we consider fast magnetosonic waves propagating toward the neutral region across the magnetic field, they grow and undergo rapid steepening after passing through the neutral region; i.e., shock formation is promoted by the background inhomogeneity. By the numerical computation of the above equation, the time evolution is examined for two initial disturbances, the pulse type (gaussian) and the wave train type (sinusoidal wave).

The relevance of the interactions between the magnetosonic shock waves and the neutral sheet plasma to plasma heating and to a triggering mechanism of sympathetic flares is also suggested.

1. Introduction

Plasma configurations with a region where the main component of the magnetic field reverses its direction are called 'magnetic neutral sheet' and are important in a number of geophysical and astrophsical applications, especially in models of solar flares (for example, Sweet, 1969) and in the geomagnetic tail.

It has been assumed that when a solar flare occurs, two processes take place in succession. The first process is a 'triggering mechanism', and the second is the explosive phase in which most of the energy transformation takes place within a time scale of 3×10^2 seconds. Ejection of plasma following the explosive phase may account for the observed horizontally propagating shock waves, and these shock waves may contribute to the triggering of sympathetic flares. Therefore, to understand the mechanism of the sympathetic flares, we must investigate the propagation of the magnetosonic waves, the shock formation, and the plasma heating near the neutral sheet.

The purpose of this paper is to investigate nonlinear magnetosonic waves propagating in an inhomogeneous plasma with a neutral sheet. In the previous paper (paper (I): Sakai, 1972) we considered nonlinear magnetosonic waves in a uniform plasma with an effective electrical conductivity, and showed that these waves were governed by the Burgers type equation, which has a shock solution. Inhomogeneous

effects, which were neglected in the previous work, must be considered because the shock formation is promoted by these effects.

Following a method developed by Asano and Taniuti (1969, 1970), in Section 2 we will show that the nonlinear behaviour of the magnetosonic waves is described by a 'modified Burgers equation' with an additional term due to the slowly varying density of the plasma (or to the slowly varying magnetic field). The waves will grow due to the inhomogeneous effects and thus shock formation is promoted. In Section 3, fast magnetosonic waves propagating perpendicular to the main magnetic field are examined by a numerical computation of the modified Burgers equation. Two initial disturbances are examined; the first is of gaussian form and the second is of the wave train type (sinusoidal wave). In Section 4, interactions between the magnetosonic shock waves and the neutral sheet are discussed by taking account of some dissipation mechanisms (two-stream instability and current driven instabilities) in the shock front passing through the neutral sheet. It is suggested that these interactions will lead to the plasma heating near the neutral sheet and will be responsible for the triggering mechanism of solar sympathetic flares. Finally in Section 5 the main results are summarized.

2. Physical Model and Formulation of the Equations

Recent observations of the neutral sheet in the geomagnetic tail (Schindler and Ness, 1972) show that the picture of a plane current sheet model (Figure 1 and Figure 2) is useful if one is interested in the average field structure. We here adopt the following static equilibrium model for a neutral sheet,

$$\vec{\nabla} p = (\vec{j} \times \vec{B})/c, \tag{1}$$

where P is the pressure and the current $\vec{j}$ follows from the Maxwell equation, $\vec{j} = c\vec{\nabla} \times \vec{B}/4\pi$.

Several simplifying assumptions are made. The plasma density $\rho_0(x)$ and the magnetic field $B_y^{(0)}(x)\vec{e}_y$ vary slowly in the x-direction, satisfying Equation (1), but are uniform in the y-and z-directions. The plasma is isothermal, with temperature T. Introducing the characteristic scale length $L_0 = \{d(\ell n \rho_0)/dx\}^{-1}$, which is a measure of the variation of the background inhomogeneity, the equilibrium state varies slowly compared with the characteristic magnetosonic wave length k^{-1}, i.e., $\rho_0 = \rho_0(\varepsilon x)$ and $B_y^{(0)} = B_y^{(0)}(\varepsilon x)$, where ε is a smallness parameter defined by $\varepsilon \sim (kL_0)^{-1}$.

In order to investigate magnetosonic waves propagating in the x-y plane, we start with the system of MHD equations,

$$\frac{\partial \rho}{\partial t} + \frac{\partial}{\partial x}(\rho v_x) + \frac{\partial}{\partial y}(\rho v_y) = 0, \tag{2}$$

$$\frac{\partial v_x}{\partial t} + v_x\frac{\partial v_x}{\partial x} + v_y\frac{\partial v_x}{\partial y} + \frac{1}{\rho}\frac{\partial \rho}{\partial x} + s\frac{B_y}{\rho}\left(\frac{\partial B_y}{\partial x} - \frac{\partial B_x}{\partial y}\right) = 0, \tag{3}$$

$$\frac{\partial v_y}{\partial t} + v_x\frac{\partial v_y}{\partial x} + v_y\frac{\partial v_y}{\partial y} + \frac{1}{\rho}\frac{\partial \rho}{\partial y} - s\frac{B_x}{\rho}\left(\frac{\partial B_y}{\partial x} - \frac{\partial B_x}{\partial y}\right) = 0, \tag{4}$$

$$\frac{\partial B_x}{\partial t} - \frac{\partial}{\partial y}(v_x B_y - v_y B_x) - D_m\left(\frac{\partial^2 B_x}{\partial x^2} + \frac{\partial^2 B_x}{\partial y^2}\right) = 0, \tag{5}$$

$$\frac{\partial B_y}{\partial t} + \frac{\partial}{\partial x}(v_x B_y - v_y B_x) - D_m\left(\frac{\partial^2 B_y}{\partial x^2} + \frac{\partial^2 B_y}{\partial y^2}\right) = 0, \tag{6}$$

$$s = \frac{1}{c_s^2}\frac{B^2(\infty)}{4\pi\rho(0)}, \tag{7}$$

$$D_m = \frac{c^2}{4\pi\,\sigma_{eff}\,c_s\,L_0}, \tag{8}$$

where the following normalization have been used,

$$\rho = \tilde{\rho}/\rho_{(0)}, \quad \vec{v} = \vec{\tilde{v}}/c_s, \quad \vec{B} = \vec{\tilde{B}}/B(\infty),$$

$$t = c_s\tilde{t}/L_0, \quad \vec{x} = \vec{\tilde{x}}/L_0, \quad \vec{x}(x, y).$$

The quantities with the superscript tilde mean the appropriate unnormalized quantities. $\rho(0)$ is the plasma density at $x=0$, and $B(\infty)$ is the magnetic field at $x=\infty$. In Equation (8) the effective electrical conductivity σ_{eff} has been introduced.

To examine slow variation of the amplitude of the magnetosonic waves, it is appropriate to introduce the following new variables (ξ,η) through the stretching

$$\xi = \int k_x dx + k_y y - \omega t, \tag{9}$$

$$\eta = \varepsilon x. \tag{10}$$

At the same time, we expand the dependent variables around the equilibrium state $\rho_0(\varepsilon x)$ and $B_y^{(0)}(\varepsilon x)$, as a power series in ε:

$$\rho = \rho_0 + \varepsilon\rho_1 + \varepsilon^2\rho_2 + \cdots, \tag{11}$$

$$v_x = 0 + \varepsilon v_{x1} + \varepsilon^2 v_{x2} + \cdots, \tag{12}$$

$$v_y = 0 + \varepsilon v_{y1} + \varepsilon^2 v_{y2} + \cdots, \tag{13}$$

$$B_x = 0 + \varepsilon B_{x1} + \varepsilon^2 B_{x2} + \cdots, \tag{14}$$

$$B_y = B_y^{(0)} + \varepsilon B_{y1} + \varepsilon^2 B_{y2} + \cdots \tag{15}$$

We wish to examine Equations (2) ~ (6) for solutions in terms of the variables (ξ,η). These procedure is the same as that of paper (I) apart from the complexity of calculations (see Appendix (A)).

We obtain the following dispersion relation for the magnetosonic waves, which is determined by the local plasma density $\rho_0(\eta)$ and the local magnetic field $B_y^{(0)}(\eta)$

$$\omega^4 - \omega^2 k^2 (1 + v_{a_0}^2(\eta)) + k^2 k_y^2 \, v_{a_0}^2(\eta) = 0, \tag{16}$$

where $k^2 = k_x^2 + k_y^2$ and $v_{a_0}^2(\eta) = s \, B_y^{(0)^2}(\eta)/\rho_0(\eta)$. After some manipulation, we obtain a modified Burgers equation for the wave amplitude $\phi(\xi,\eta)$:

$$\frac{\partial \phi}{\partial \eta} + a(\eta)\phi\frac{\partial \phi}{\partial \xi} - b(\eta)\frac{\partial^2 \phi}{\partial \xi^2} + c(\eta)\phi = 0, \tag{17}$$

where $a(\eta)$, $b(\eta)$ and $c(\eta)$ are given by

$$a(\eta) = \frac{[\{1+(k_y^2/\omega^2-1)/2+v_{a_0}^2(k_y^2/\omega^2-1)^2\}k_x^2+(\omega^2/2+k_y^2 v_{a_0}^2)(k_y^2/\omega^2-1)^2]}{2k_x(k_y^2/\omega^2-1)\{v_{a_0}^2(k_y^2/\omega^2-1)-1\}}, \tag{18}$$

$$b(\eta) = \frac{D_m(k_x^2+k_y^2)^2 v_{a_0}^2(k_y^2/\omega^2-1)}{2\omega k_x\{v_{a_0}^2(k_y^2/\omega^2-1)-1\}}, \tag{19}$$

$$c(\eta) = \alpha(\eta)\frac{1}{\rho_0}\frac{d\rho_0}{d\eta}, \tag{20}$$

$$\alpha(\eta) = \frac{(v_{a_0}^2+4)\omega^4 - 2\omega^2 k_y^2(v_{a_0}^2+2)+4v_{a_0}^2 k_y^4}{4(\omega^2-v_{a_0}^2 k_y^2)\{v_{a_0}^2 k_y^2 - \omega^2(1+v_{a_0}^2)\}}. \tag{21}$$

In Equation (17), the second term and the third term represent the nonlinearity and the effect of dissipation

due to the effective electrical conductivity, respectively. The last term represents the effect of the plasma inhomogeneity. This equation is to be compared with the well-known Burgers equation, in which coefficients a and b are constant and the last term is not present. We shall, therefore, refer to Equation (17) as the 'modified Burgers equation'.

It is difficult to solve the above modified Burgers equation under any given plasma model, but we can investigate the problem of how the background inhomogeneity affects wave propagation. If one neglects dissipation effects ($D_m \to 0$), then we can integrate the equation by the method of characteristic (Asano and Taniuti, 1969). The wave amplitude is given by

$$\phi(\xi,\eta) = \phi_0 \mathrm{EXP}\left(-\int_{\eta_0}^{\eta} c(\eta)d\eta\right), \tag{22}$$

along the characteristics defined by the equation

$$\frac{d\xi}{d\eta} = a(\eta)\phi(\xi,\eta), \tag{23}$$

where ϕ_0 is the wave amplitude at $\eta=\eta_0$. From Equation (22), we find that if $\int_{\eta_0}^{\eta} c(\eta)d\eta$ is negative, the waves grow along the characteristics. This means that the inhomogeneous effect promotes shock formation.

3. Fast Magnetosonic Waves passing through a Neutral Sheet

In the previous section we derived the modified Burgers

equation which governs nonlinear magnetosonic wave propagation in a plasma with a slow variation of the background. We here investigate only the fast magnetosonic waves propagating perpendicular to the magnetic field in a plasma with a neutral sheet. We assume that the plasma with the neutral sheet is described by the following density and magnetic field, which are also solutions in static equilibrium:

$$\rho_0(\eta) = \mathrm{sech}^2(\eta), \tag{24}$$

$$B_y^{(0)}(\eta) = \tanh(\eta). \tag{25}$$

In the case of the fast magnetosonic wave, the coefficients of the modified Burgers equation (17) reduce to

$$a(\eta) = \frac{\omega_+(2 + 3\, v_{a_0}^2)}{4(1 + v_{a_0}^2)^{3/2}}, \tag{26}$$

$$b(\eta) = \frac{D_m\, \omega_+^2\, v_{a_0}^2}{2(1 + v_{a_0}^2)^{5/2}}, \tag{27}$$

$$c(\eta) = -\frac{(4 + v_{a_0}^2)}{4(1 + v_{a_0}^2)} \frac{1}{\rho_0} \frac{d\rho_0}{d\eta}, \tag{28}$$

where we have used the following dispersion relation for the fast magnetosonic wave,

$$\omega_+^2 = k_+^2(1 + v_{a0}^2), \tag{29}$$

where the subscript '+' is used for definiteness. Substituting Equations (24) and (25) into Equations (26)~(28), we obtain

$$a(\eta) = \frac{\omega_+[2 + 3\mathrm{stanh}^2(\eta)\cosh^2(\eta)]}{4[1 + \mathrm{stanh}^2(\eta)\cosh^2(\eta)]^{3/2}}, \tag{30}$$

$$b(\eta) = \frac{D_m\omega_+^2\mathrm{stanh}^2(\eta)\cosh^2(\eta)}{2[1 + \mathrm{stanh}^2(\eta)\cosh^2(\eta)]^{5/2}}, \tag{31}$$

$$c(\eta) = \frac{\tanh(\eta)[4 + \mathrm{stanh}^2(\eta)\cosh^2(\eta)]}{2[1 + \mathrm{stanh}^2(\eta)\cosh^2(\eta)]}. \tag{32}$$

The η dependency of these coefficients is shown in Figure 3, and approximate forms near $\eta=0$ are given by $a(\eta)\cong\omega_+/2$, $b(\eta)\cong D_m\omega_+^2 s\eta^2/2$, and $c(\eta)\cong 2\eta$.

We show some results of the numerical computation of the modified Burgers equation (17), solved by the use of a finite difference method (Appendix.B). Two initial perturbations are examined: the first is the pulse type; $\phi_0(\xi,\eta=-\eta_0)=\mathrm{EXP}(-\xi^2)$; the second one is the wave train, $\phi_0(\xi,\eta=-\eta_0)=\mathrm{SIN}(\xi)$. The second case was solved under periodic boundary conditions for ξ; i.e., we assumed that $\phi(\xi)=\phi(\xi+2\pi)$.

Consider the magnetosonic waves excited at $\eta=-2.0$ (see Figure 2), having the form of a gaussian and a wave train in the frame moving with the local phase velocity (the wave

frame). These waves propagate in the positive x-direction, across the main magnetic field $B_y^{(0)}$. The wave speed is approximately determined by the local phase velocity $v_{ph}=(c_s^2+v_a^2)^{1/2}$, which decreases until $\eta=0$, and then again increases in the positive x-direction. When the waves approach the region of the null magnetic field, the compression effect of waves occurs, because the wave speed becomes slower. At the same time, the compression effect is promoted by the inhomogeneity, and shock formation becomes more rapid (see Figure 4 ~ Figure 7).

The following parameters have been used: (a) $s=B^2(\infty)/4\pi\rho(0)C_s^2=1$, which is derived from Equation (1) with use of Equations (24) and (25); (b) $\omega_+=\omega/(c_s/L_0)=0.1$, 0.3 and 0.5, which correspond to $10^{-2}\omega_{ci}\lesssim\omega\lesssim10^{-1}\omega_{ci}$ for solar corona parameters, $B(\infty)\sim10^2$G, $T\sim10^6$K; and (c) $D_m=c^2/4\pi\sigma_{eff}c_sL_0\sim\varepsilon=0.1$, from which we obtain $\sigma_{eff}=c^2/4\pi c_sL_0\varepsilon\simeq10^{14}/L_0$.

As shown in Figure 4 and Figure 6, in the case of $\omega_+=0.1(\omega\sim10^{-2}\omega_{ci})$, we find that the steepening effect is rather weak as compared with the other cases of $\omega_+=0.3$ and 0.5. Even for a very weak dissipation effect $D_m\sim(10^{-2}\sim10^{-5})$, we find from numerical results that the wave pattern is the same as in Figure 4 and Figure 6, and the steepness is also weak. However, as the frequency ω increases, then the wave length decreases, the steepening effect becomes stronger (Figure 5 and Figure 7), and leads to shock formation.

We here note the Alfvén Mach number of these waves ($k_y=0$). From Equations (9) and (10), we obtain

$$\frac{dx}{dt} = \frac{\omega}{k_x}\left[1 - \frac{\varepsilon}{k_x}\frac{d\xi}{d\eta}\right]^{-1}. \tag{33}$$

In the laboratory frame, this reduces to

$$\frac{dx}{dt} \cong (c_s^2 + v_a^2)^{1/2}\left(1 + \frac{\varepsilon}{k_x}\frac{d\xi}{d\eta}\right). \tag{34}$$

Using Equation (23), we obtain the Alfvén Mach number as

$$M_a = \frac{dx/dt}{v_a} = \{1 + (c_s/v_a)^2\}^{1/2}[1 + \varepsilon\{1+v_{a_0}^2\}^{1/2} a(\eta)\phi/\omega_+], \tag{35}$$

which is determined by the local plasma parameters and the wave amplitude $\phi(\xi,\eta)$.

4. Neutral Sheet Plasma Heating by Magnetosonic Shock

In the preceding sections we have shown that magnetosonic waves passing through the neutral sheet steepen and become shock-like due to nonlinear effects and background inhomogeneity. So far, we have simply expressed the effects of any micro-instabilities by an effective electrical conductivity σ_{eff} without discussing these in detail. We now discuss some dissipation mechanisms near the magnetosonic shock front and the resultant plasma heating by the magnetosonic shock waves.

Let us consider the situation where the magnetosonic shock wave propagates through the neutral sheet, and a shock

front of width L exists near the sheet (Figure 8). A diamagnetic current is produced by the magnetic field gradients ∇B near the shock front. The diamagnetic current gives rise to a two-stream instability and some current-driven instabilities [for example, Tidmann and Krall, 1971]. The two-stream instability will be excited under the condition that the drift velocity v_d produced by the magnetic field gradient exceeds the electron thermal velocity v_{th}, and the current-driven instabilities associated with unstable ion acoustic waves and unstable electron Bernstein modes will be excited under the condition $v_d > c_s = (m_e/m_i)^{1/2} v_{th} \sim v_{th}/43$, which is weaker than that the two-stream instability. The drift velocity v_d can be estimated from the Maxwell equation $\vec{\nabla} \times \vec{B} = 4\pi \vec{j}/c$ as

$$v_d \sim (c/4\pi ne)(dB/dx). \tag{36}$$

Then the condition for the excitation of the two-stream instability, $v_d > v_{th}$ becomes

$$\varepsilon/L > (v_{th}/c^2)(\omega_{pe}^2/\omega_{ce}^*), \tag{37}$$

where $\varepsilon = B/B(\infty)$ is the shock wave amplitude normalized by the magnetic field $B(\infty)$, ω_{pe} is the plasma frequency, and $\omega_{ce}^* = eB(\infty)/m_e c$. From the result of some laboratory experiments [for example, Paul, 1972], the width L may be estimated to be as $L \sim \alpha c/\omega_{pe}$, where α is a numerical factor and of value

in the range 1~10 [Appendix C]. Using $L \sim \alpha c/\omega_{pe}$, we obtain the criterion of the two-stream instability from Equation (37) to be

$$\varepsilon \equiv (B/B(\infty)) > \alpha (v_{th}/c)(\omega_{pe}/\omega_{ce}^{*}) \equiv \varepsilon_c . \tag{38}$$

We must also consider another criterion, that the above instabilities can grow enough in the shock front. This condition is that the maximum growth rate γ_m of the instabilities must be large compared with the inverse of the transit time τ_{tr} during which the shock front passes through the scale of the front width; i.e., $\gamma_m \tau_{tr} > 1$. Since $v_a \lesssim c_s$ in the neutral region, we can estimate the transit time τ_{tr}

$$\tau_{tr} \sim L/c_s \sim \alpha (c/\omega_{pe} c_s) . \tag{39}$$

For parameters of the solar corona, say, $B(\infty) \sim 10G$, $n \sim 10^8 cm^{-3}$, $T \sim 10^2 ev$ and $\alpha \sim 1$, we have $\varepsilon_c \sim 0.1$ from Equation (38) and $\tau_{tr} \sim 4 \times 10^{-6} sec$ from Equation (39). From $\gamma_m \tau_{tr} > 1$ the maximum growth rate γ_m must be $\gamma_m > 2.5 \times 10^5 \ sec^{-1} \omega_{ce}/40$ for $\varepsilon \gtrsim \varepsilon_c \sim 0.1$.

Among the instabilities due to diamagnetic current, the two-stream instability is strongest, and its maximum growth rate γ_m equals $(m_e/m_i)^{1/3} \omega_{pe} \sim 10^7 sec^{-1}$. The current driven instabilities associated with unstable ion acoustic waves and unstable electron Bernstein modes have maximum growth rate $\gamma_m \sim (10^{-1} \sim 10^{-2}) \omega_{ce}$ [for example, Lashmore-Davies,

1971]. Therefore the two-stream instability and the current driven instabilities will probably be responsible for dissipation of the magnetosonic shock front near the neutral sheet.

Next we consider how much the neutral sheet plasma is heated by the magnetosonic shock waves. The scheme of energy flow is supposed that the energy of the shock waves is partially transformed into the energy of the unstable modes excited near the shock front and into thermal energy of the neutral sheet plasma by turbulent ohmic dissipation. The change of the drift energy is given by

$$\frac{d}{dt}\left(\frac{m_i}{2} n v_d^2\right) = - m_i n v_d \frac{dv_d}{dt} . \qquad (40)$$

Using Equation (36) and the relation $L \sim \alpha / c\omega_{pe}$, we obtain

$$\frac{m_i n}{2} v_d^2 \cong \frac{m_i}{\alpha m_e} \varepsilon_B , \qquad (41)$$

where ε_B is the density of the shock wave, $\varepsilon_B = B^2/8\pi$. We obtain $\varepsilon_B \sim 2.5 \times 10^{10}$ eV, and drift energy $m_i n v_d^2/2 \sim 4.5 \times 10^{12}$ eV (we put $\alpha = 1$), for the magnetic field intensity of the shock of the order of one gauss, which is 1/500 of the sun spot magnetic field intensity. A portion of this drift energy will be transformed into plasma thermal energy. Introducing the efficiency η_e of transformation from drift energy to

thermal energy ($\eta_e<1$), we expect the resultant temperature to be

$$T \sim \eta_e \frac{4.5 \times 10^{12}}{n} \text{ (eV)}. \tag{42}$$

For example, if we take $n \sim 10^8$ cm^{-3}, $\eta_e \sim 0.01$, then we obtain $T \sim 450$ eV, which is about 4.5 times higher than the temperature of the solar corona $T_0 \sim 10^2$eV. The unknown parameter η_e must be determined by taking account of the nonlinear saturation mechanisms of the above instabilities, which remain as future problems.

From these discussions, the magnetosonic shock waves passing through the neutral sheet plasma will produce the turbulence generated by the two-stream instability and current driven instabilities, and the resultant effective electrical conductivity near the neutral sheet will be reduced by the scattering between the turbulence generated by the magnetosonic shock waves and electrons maintaining the neutral sheet current. Then the magnetic field produced by the neutral sheet current will be dissipated by the turbulent ohmic dissipation induced by the passing of the magnetosonic shock waves. These processes will be responsible for a triggering mechanism for the sympathetic flares.

5. Conclusions

Our main conclusions are summarized as follows.

(1) Nonlinear behaviour of magnetosonic waves propagating in a weakly inhomogeneous plasma governed by the equations of static equilibrium (Equation (1)) is found to be described by a modified Burgers equation (17).

(2) The fast magnetosonic waves passing through the neutral sheet grow and undergo rapid steepening and shock formation is promoted by the plasma inhomogeneity. In the low frequency region, the steepening effect is weak, but in the higher frequency region the steepening effect becomes stronger.

(3) The magnetosonic shock waves passing through the neutral sheet plasma will produce turbulence as a result of the two-stream instability and current driven instabilities, and the effective electrical conductivity will be reduced. Then, due to turbulent ohmic dissipation, the magnetic field energy will be also reduced. It is suggested that these successive processes may be responsible for triggering of the sympathetic flares.

Acknowledgements

The author wishes to thank Professor Y. Terashima for reading the original manuscript. He is also grateful to Professor T. Taniuti and Dr N. Asano for useful discussions, and to Mr Van Dam for correcting the English. Numerical calculations were carried out by HITAC 8500 computer system of the Institute of Plasma Physics.

Appendix (A)

We obtain the following equation for order ε.

$$A_0 \frac{\partial U^{(1)}}{\partial \xi} = 0, \tag{A-1}$$

where A_0 and $U^{(1)}$ are a 5×5 matrix and a column vector, respectively. The components of A_0 and $U^{(1)}$ are defined as follows;

$$A_0 = \begin{pmatrix} -\omega & k_x\rho_0 & k_y\rho_0 & 0 & 0 \\ k_x/\rho_0 & -\omega & 0 & -sk_yB_y^{(0)}/\rho_0 & sk_xB_y^{(0)}/\rho_0 \\ k_y/\rho_0 & 0 & -\omega & 0 & 0 \\ 0 & -k_yB_y^{(0)} & 0 & -\omega & 0 \\ 0 & k_xB_y^{(0)} & 0 & 0 & -\omega \end{pmatrix} \tag{A-2}$$

$$U^{(1)} = \begin{pmatrix} \rho_1 \\ v_{x_1} \\ v_{y_1} \\ B_{x_1} \\ B_{y_1} \end{pmatrix}. \tag{A-3}$$

Det $A_0=0$ yields the local dispersion relation, Equation (16) for magnetosonic waves. The solution of Equation (A-1) can be written as

$$U^{(1)}(\xi,\eta) = R(\eta)\phi(\xi,\eta), \tag{A-4}$$

where R is a column vector satisfying

$$A_0 R = 0. \tag{A-5}$$

We obtain from Equation (A-5)

$$R = \begin{pmatrix} \rho_0 \\ \omega(k_y^2/\omega^2 - 1)/k_x \\ -k_y/\omega \\ k_y B_y^{(0)} (k_y^2/\omega^2 - 1)/k_x \\ -B_y^{(0)} (k_y^2/\omega^2 - 1) \end{pmatrix} \tag{A-6}$$

From Equation L $A_0=0$, where L is a row vector corresponding R, we also obtain

$$L=[1,\rho_0\omega(k_y^2/\omega^2-1)/k_x,-k_y\rho_0/\omega,\ sk_yB_y^{(0)}(k_y^2/\omega^2-1)/k_x,-sB_y^{(0)}(k_y^2/\omega^2-1)] \tag{A-7}$$

From the second order, we have the equation,

$$A_0\frac{\partial U^{(2)}}{\partial\xi}=B\ , \tag{A-8}$$

where B and $U^{(2)}$ are column vectors;

$$U^{(2)}=\begin{pmatrix}\rho_2\\ v_{x_2}\\ v_{y_2}\\ B_{x_2}\\ B_{y_2}\end{pmatrix} \tag{A-9}$$

$$B=\begin{pmatrix}b_1\\ b_2\\ b_3\\ b_4\\ b_5\end{pmatrix}$$

$$b_1=-k_x\frac{\partial}{\partial\xi}(\rho_1 v_{x_1})-k_y\frac{\partial}{\partial\xi}(\rho_1 v_{y_1})-\frac{\partial}{\partial\eta}(\rho_0 v_{x_1}),$$

$$b_2=-k_x v_{x1}\frac{\partial v_{x_1}}{\partial\xi}-k_y v_{y_1}\frac{\partial v_{x_1}}{\partial\xi}-\frac{1}{\rho_0}\frac{\partial\rho_1}{\partial\eta}+k_x\frac{\rho_1}{\rho_0^2}\frac{\partial\rho_1}{\partial\xi}+\frac{\rho_1}{\rho_0^2}\frac{\partial\rho_0}{\partial\eta}-B_y^{(0)}\frac{s}{\rho_0}\frac{\partial B_{y_1}}{\partial\eta}$$
$$-\frac{s}{\rho_0}(B_{y_1}-\frac{\rho_1 B_y^{(0)}}{\rho_0})(k_x\frac{\partial B_{y_1}}{\partial\xi}+\frac{\partial B_y^{(0)}}{\partial\eta}-k_y\frac{\partial B_{x_1}}{\partial\xi}),$$

$$b_3=-k_x v_{x1}\frac{\partial v_{y_1}}{\partial\xi}-k_y v_{y1}\frac{\partial v_{y_1}}{\partial\xi}+\frac{\rho_1}{\rho_0^2}k_y\frac{\partial\rho_1}{\partial\xi}+\frac{s}{\rho_0}B_{x_1}(k_x\frac{\partial B_{y_1}}{\partial\xi}-k_y\frac{\partial B_{x_1}}{\partial\xi}+\frac{\partial B_y^{(0)}}{\partial\eta}),$$

$$b_4=k_y\frac{\partial}{\partial\xi}(v_{x_1}B_{y_1})-k_y\frac{\partial}{\partial\xi}(v_{y_1}B_{x_1})+D_m(k_x^2+k_y^2)\frac{\partial^2 B_{x_1}}{\partial\xi^2},$$

$$b_5=-k_x\frac{\partial}{\partial\xi}(v_{x_1}B_{y_1})-\frac{\partial}{\partial\eta}(v_{x_1}B_y^{(0)})+k_x\frac{\partial}{\partial\xi}(v_{y_1}B_{x_1})+D_m(k_x^2+k_y^2)\frac{\partial^2 B_{y_1}}{\partial\xi^2}.$$

We multiply Equation (A-8) by the left eigenvector L, substituting Equation (A-4) and Equation (A-6) into Equation (A-8) at the same time. From LB=0, we obtain the modified Burgers equation (17).

Appendix (B)

We describe the finite difference method used for solving the modified Burgers equation (17). The following differences were used:

$$\partial\phi/\partial\eta = (\phi_{i+1,j} - \phi_{i,j})/\Delta\eta \ , \tag{B-1}$$

$$\partial\phi/\partial\xi = (\phi_{i,j+1} - \phi_{i,j-1})/2\Delta\xi \ , \tag{B-2}$$

$$\phi = (\phi_{i,j+1} + \phi_{i,j-1})/2 \ , \tag{B-3}$$

$$\partial^2\phi/\partial\xi^2 = (\phi_{i,j+1} - 2\phi_{i,j} + \phi_{i,j-1})/(\Delta\xi)^2 \ . \tag{B-4}$$

In order to obtain $\phi_{i+1,j}$, we have used the values at i for the coefficients a, b, and c. We note that the stability condition for the diffusion equation exists approximately at each point of η, i.e.,

$$2b(\Delta\eta)/(\Delta\xi)^2 \lesssim 1, \text{ for } \frac{\partial\phi}{\partial\eta} = b\frac{\partial^2\phi}{\partial\xi^2} \ . \tag{B-5}$$

We define the following quantity I

$$I = \int_{-\infty}^{\infty} \phi(\xi,\eta)d\xi \ . \tag{B-6}$$

Integrating Equation (17) from $-\infty$ to ∞ with respect to ξ,

and using $\phi(\xi=\pm\infty)=0, \partial\phi/\partial\xi\Big|_{\xi=\pm\infty} = 0$, we obtain

$$\frac{\partial I}{\partial \eta} + c(\eta) I = 0. \tag{B-7}$$

The solution of Equation (B-7) is

$$I(\eta) = I_0 EXP\left(- \int_{-\eta_0}^{\eta} c(\eta) d\eta \right), \tag{B-8}$$

where I_0 is the value of I at $\eta=-\eta_0$. When $C(\eta)$ is an odd function and $\eta=\eta_0$, we obtain $I=I_0$; i.e., the quantity I is conserved. The fact that quantity I is conserved is used to check the accuracy of the above finite difference method.

Appendix C

In paper (I), we derived the shock front thickness L in the case of the fast mode,

$$L \sim \left(\frac{c}{\omega_{pe}}\right)^2 \frac{\nu_{eff}}{v_0} \frac{1}{(1+\beta^2)} , \qquad (C\text{-}1)$$

where v_0 is the front velocity, ν_{eff} the effective collision frequency, and $\beta=(c_s/v_a)$.

If the two-stream instability may be responsible for dissipation of the magnetosonic shock, we can estimate the width L, using the relation that the effective collision frequency ν_{eff} equals the maximum growth rate $\gamma_m \sim (m_e/m_i)^{1/3}\omega_{pe}$, as

$$L \sim \left(\frac{m_e}{m_i}\right)^{1/3} \left(\frac{c}{v_0}\right) \left(\frac{1}{1+\beta^2}\right) \left(\frac{c}{\omega_{pe}}\right) \equiv \alpha \frac{c}{\omega_{pe}} , \qquad (C\text{-}2)$$

where $\alpha=(m_e/m_i)^{1/3}\ (c/v_0)(1+\beta^2)^{-1}$ is a numerical factor and approximately of value in the range 1 ~ 10.

References

Asano, N. and Taniuti, T.: 1969, J. Phys. Soc. Japan 27, 1059.
1970, J. Phys. Soc. Japan 29, 209.

Lashmore-Davies, C.N.: 1971, Phys. Fluids 14, 1481.

Paul, J.W.M.: 1972, 'Collisionless shocks' in Cosmic Plasma Physics, edited by K. Schindler, p.293, Plenum Press, New York.

Sakai, J.: 1972, Cosmic Electrodynamics 3, 260.

Schindler, K. and Ness, N.F.: 1972, Jour. Geophys. Res. 77,91.

Sweet, P.A.: 1969, 'Mechanisms of Solar Flares' in Annual Review of Astronomy and Astrophysics, Vol.7, p.149.

Tidman, D.A. and Krall, N.A.: 1971, 'Shock Waves in Collisionless Plasmas' p.115, Wiley-Interscience.

Figure Captions

Fig.1 The coordinate system and magnetic field configuration in a plasma with a neutral sheet. Magnetosonic waves propagate in a x-y plane across the magnetic field.

Fig.2 Configurations for the density and the magnetic field across the neutral sheet; $\rho_0=\rho(0)\mathrm{sech}^2(\eta)$ and $B_y^{(0)}=B(\infty)\tanh(\eta)$.

Fig.3 η-dependency of coefficients $a(\eta)$, $b(\eta)$, and $c(\eta)$ of the modified Burgers equation (17), in the case of $\omega_+=0.3$, $D_m=0.1$ and $s=1.0$.

Fig.4 Evolution of an initial pulse $\phi_0(\xi,\ \eta=-2.0)=\mathrm{EXP}(-\xi^2)$, in the case of $\omega_+=0.1$ and $D_m=0.1$.

Fig.5 Evolution of an initial pulse $\phi_0(\xi,\ \eta=-2.0)=\mathrm{EXP}(-\xi^2)$, in the case of $\omega_+=0.5$ and $D_m=0.1$.

Fig.6 Evolution of an initial wave train $\phi_0(\xi,\ \eta=-2.0)=\mathrm{SIN}(\xi)$, in the case of $\omega_+=0.1$ and $D_m=0.1$.

Fig.7 Evolution of an initial wave train $\phi_0(\xi,\ \eta=-2.0)=\mathrm{SIN}(\xi)$, in the case of $\omega_+=0.3$ and $D_m=0.1$.

Fig.8 Magnetosonic shock wave near the neutral sheet. L is the width of the shock front and $L_0^{-1} \sim \frac{d}{dx}(\ell n\rho_0) \sim \frac{d}{dx}(\ell nB_y^{(0)})$.

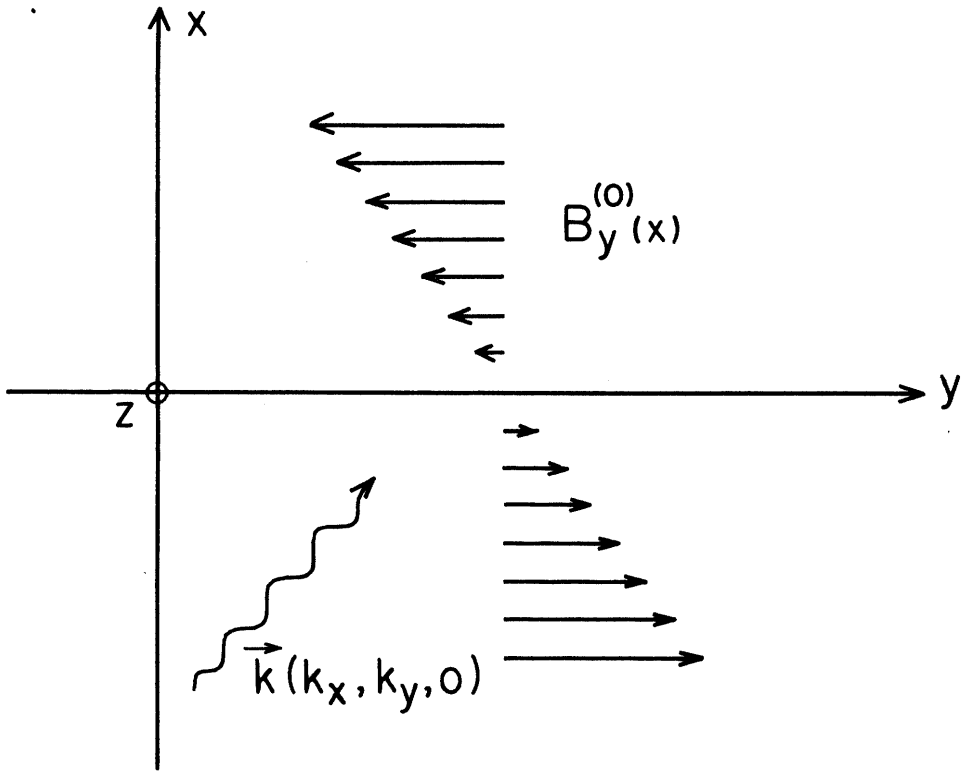

Fig. 1

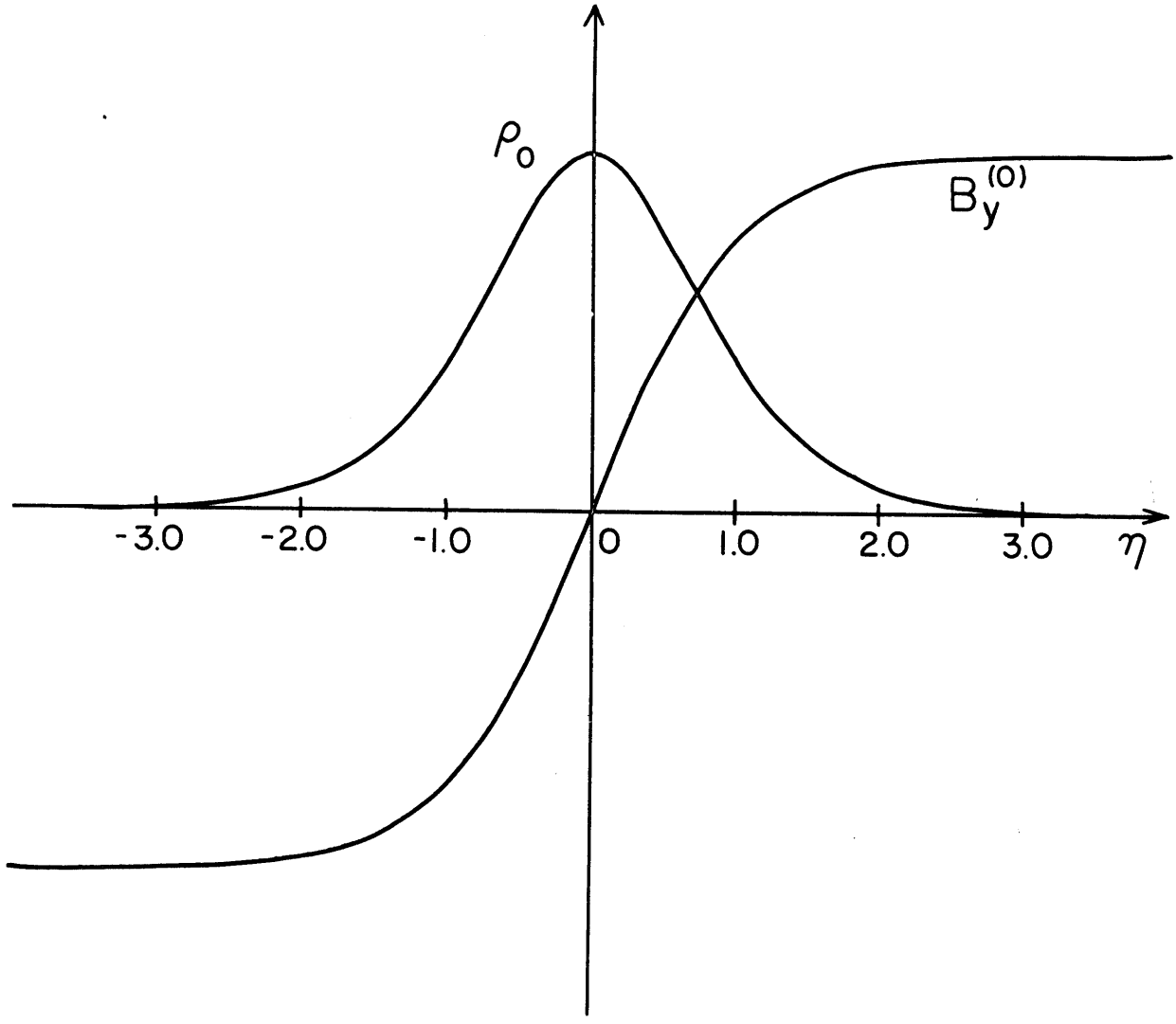

Fig. 2

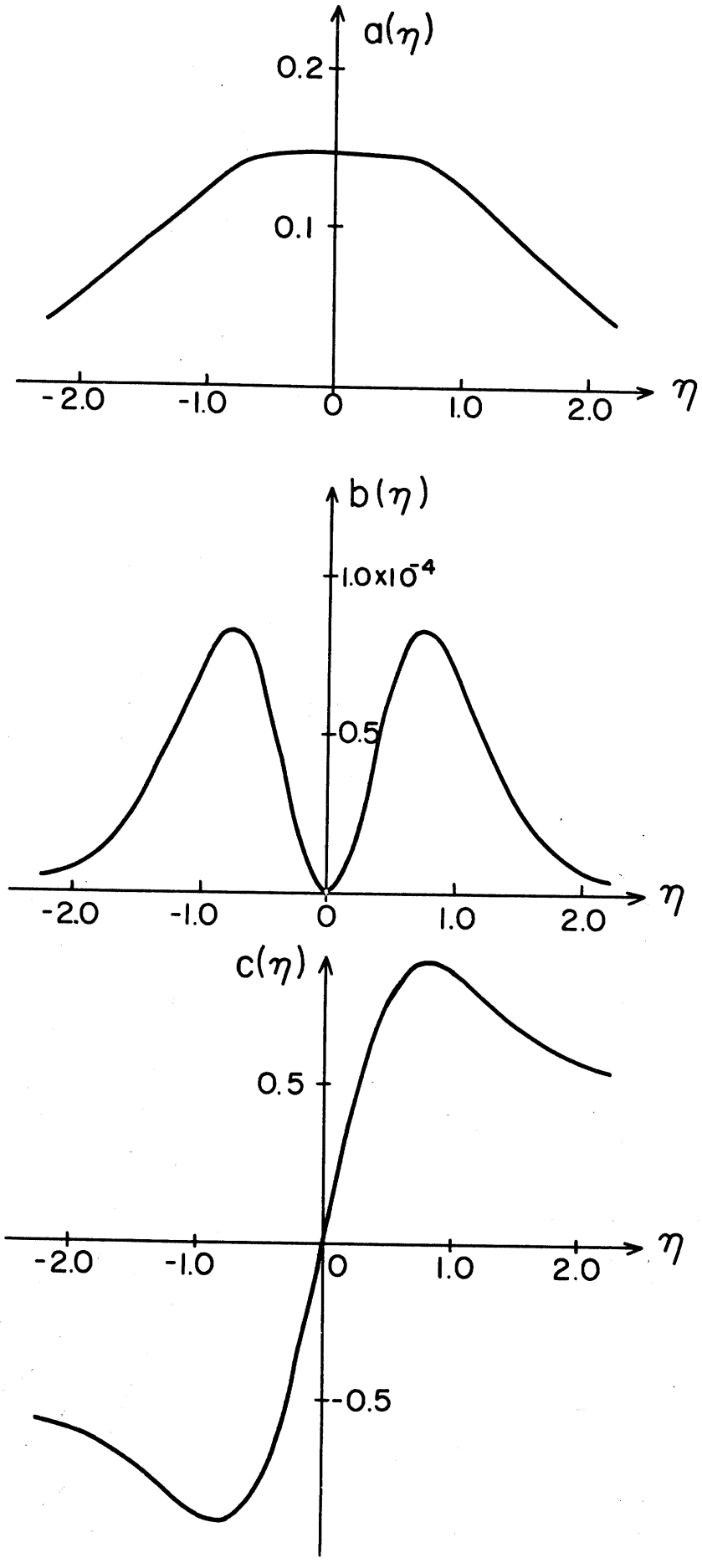
a(η)
0.2
0.1
-2.0
-1.0
0
1.0
2.0
η
b(η)
1.0x10⁻⁴
0.5
-2.0
-1.0
0
1.0
2.0
η
c(η)
0.5
-0.5
-2.0
-1.0
0
1.0
2.0
η

Fig. 3

Fig. 4

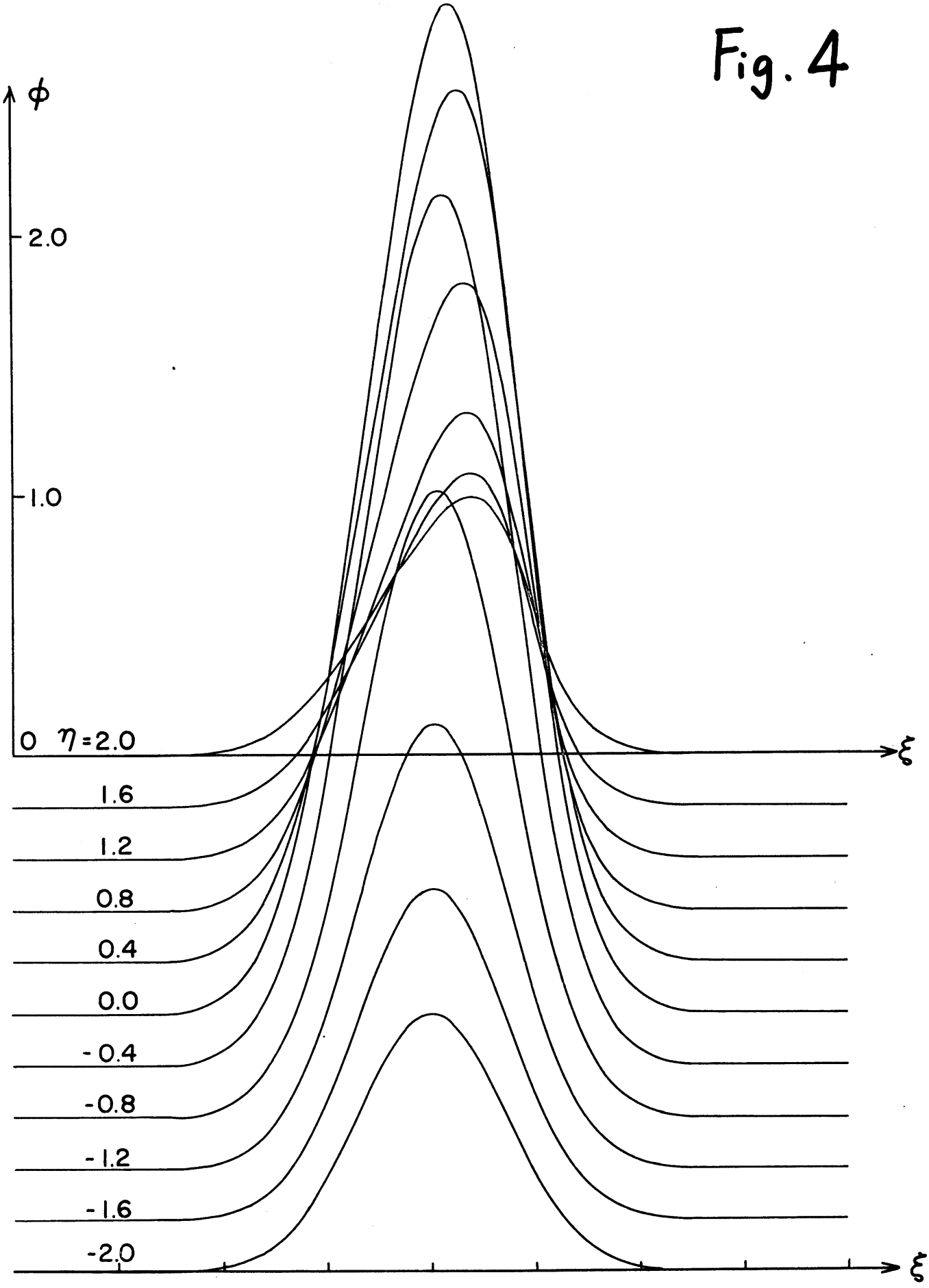

Fig. 5

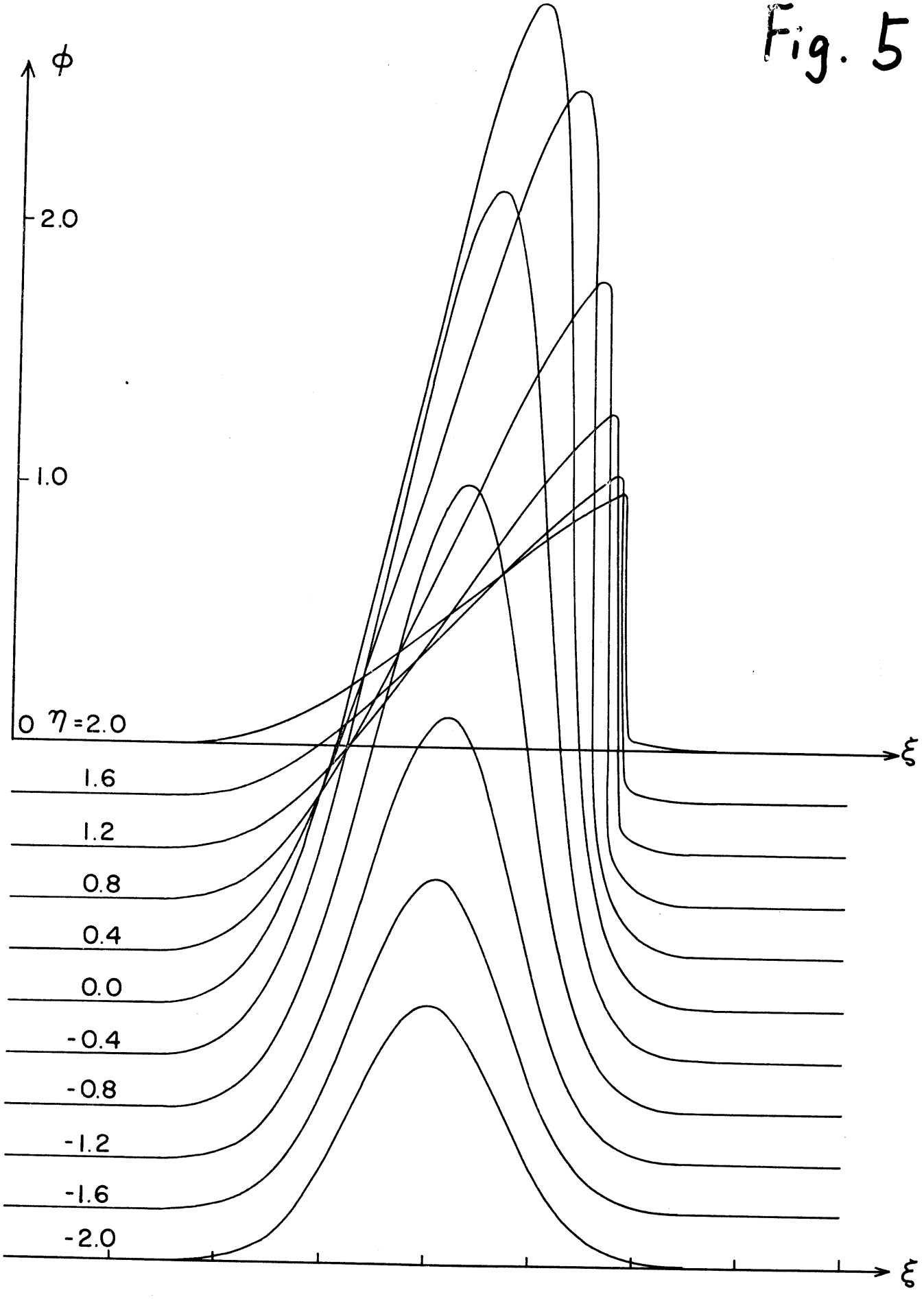

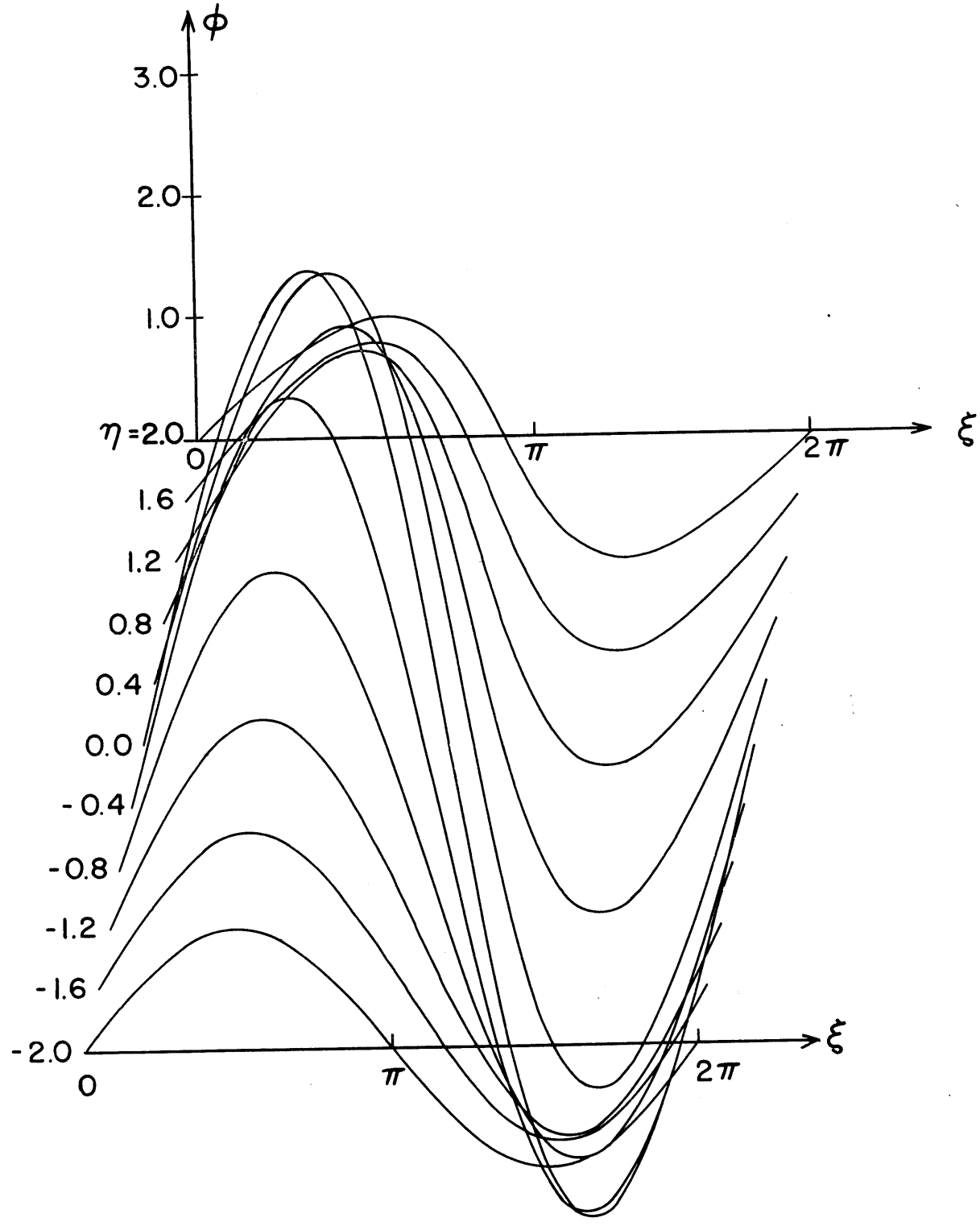

Fig. 6

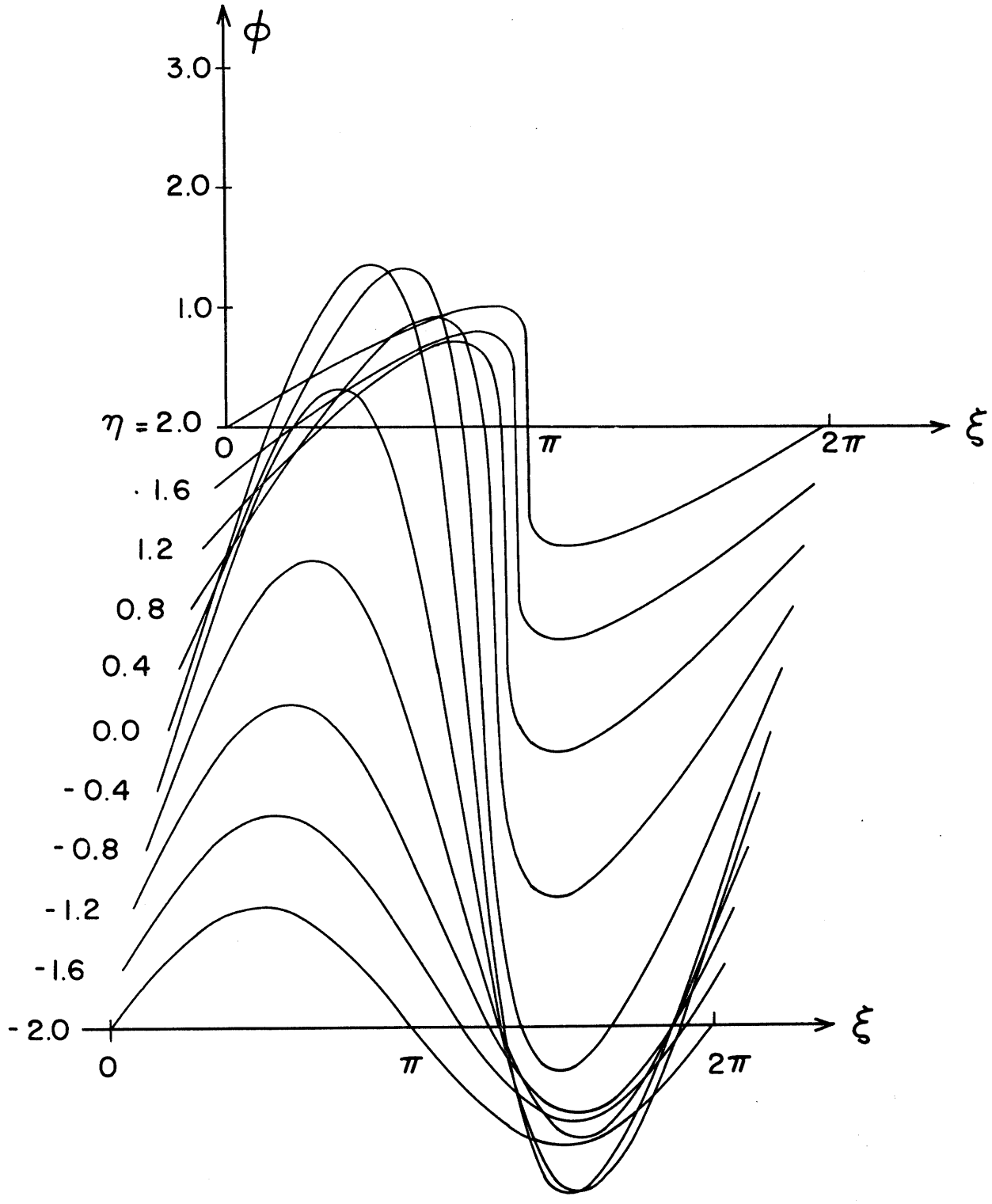

Fig. 7

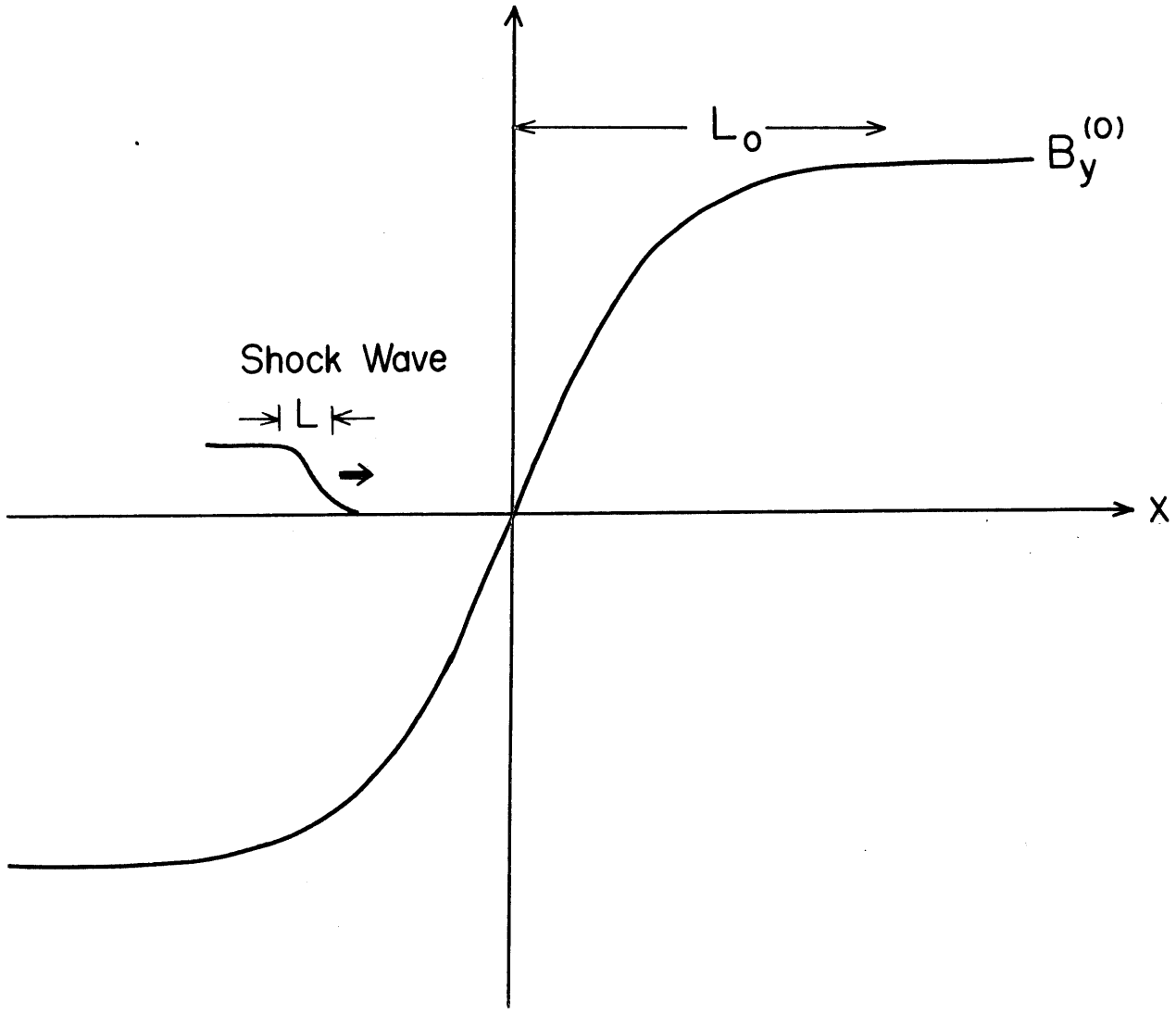

Fig. 8